

# A New Guarded Hot Plate Designed for Thermal-Conductivity Measurements at High Temperature

V. Scoarnec · J. Hameury · B. Hay

Received: 30 November 2013 / Accepted: 4 November 2014 / Published online: 18 November 2014  
© Springer Science+Business Media New York 2014

**Abstract** The Laboratoire National de Métrologie et d’Essais has developed a new guarded hot-plate apparatus operating from 23 °C to 800 °C in the thermal-conductivity range from  $0.2 \text{ W}\cdot\text{m}^{-1}\cdot\text{K}^{-1}$  to  $5 \text{ W}\cdot\text{m}^{-1}\cdot\text{K}^{-1}$ . This facility has been specifically designed for measuring medium thermal-conductivity materials at high temperature on square specimens (100 mm side), which are easier to machine than circular ones. The hot plate and cold plates are similar with a metering section independent from the guard ring. The specimens are laterally isolated by an air gap of 4 mm width and can be instrumented by temperature sensors in order to reduce effects of thermal contact resistances between the specimens and the heating plates. Measurements have been performed on certified reference materials and on “calibrated” materials. Relative deviations between thermal conductivities measured and reference values are less than 5 % in the operating range.

**Keywords** Guarded hot plate · High temperature · Metrology · Solid materials · Thermal conductivity

## 1 Introduction

Thermal-conductivity measurements of insulating materials used in building applications, performed using the guarded hot-plate (GHP) method in accordance with the standards EN 12667 [1] or ISO 8302 [2], are usually limited to the temperature range from  $-20 \text{ °C}$  to  $80 \text{ °C}$ . This well-known steady-state technique gives the lowest uncertainty (better than 1 %) for thermal-conductivity measurements on

---

V. Scoarnec · J. Hameury · B. Hay (✉)  
Laboratoire National de Métrologie et d’Essais (LNE), 75015 Paris, France  
e-mail: bruno.hay@lne.fr

low conducting materials. Thermal-conductivity measurements at higher temperatures using a GHP are rather unusual although the principle of the technique is valid whatever the temperature range. Experience shows indeed that the design, construction, and operation of a GHP apparatus at high temperatures are very challenging tasks [3]. There are, for example, design issues linked to the long-term stability of heating plates material and of temperature sensors; some hot spots can appear on the heating plates (due to non-uniformity of the heater) and can then induce errors on temperature measurements; and corrections due to heat flow across the air gap increases due to radiation heat exchanges. Actually, all the international comparisons of thermal-conductivity measurements at high temperatures that have been carried out so far have given quite large discrepancies of results (about 10 % to 15 %) [4,5], compared to 5 % and 7 % given in the standard CEN/TS 15548-1 [6] as achievable uncertainties up to 450 °C and at temperatures above 450 °C, respectively.

Reliable values of thermal properties of new advanced materials (refractory alloys, thermal protection materials, and ceramics) at high temperatures are required in many fields of industry (aerospace, energy, and transportation) in order to improve energy efficiency and to demonstrate the performance of these materials. In order to meet these needs, the Laboratoire National de Métrologie et d'Essais (LNE) has extended the temperature range of its facilities devoted to thermal property measurements [7,8], especially by developing a new guarded hot-plate apparatus adapted for thermal-conductivity measurements at high temperature. The device operates from 23 °C to 800 °C for materials having a thermal conductivity from  $0.2 \text{ W}\cdot\text{m}^{-1}\cdot\text{K}^{-1}$  to  $5 \text{ W}\cdot\text{m}^{-1}\cdot\text{K}^{-1}$ . The hot plate and the two cold plates are electrically heated and are designed with an independent metering section and a guard ring. The plates are made of high purity nickel in order to have good resistance to oxidation and a quite high thermal conductivity to ensure a good uniformity of temperature. Their thickness has been increased to improve the temperature uniformity and their resistance to distortion under load at high temperature due to their own weight. The guard rings are as wide as the metering area, enabling a reduction of the thermal flux disturbances around the samples. Measurements can be performed in a single or double-specimen configurations using small square specimens ( $100 \text{ mm} \times 100 \text{ mm}$ ), which are usually easier to machine than circular samples. Holes can be drilled in the specimens in order to introduce temperature sensors enabling direct measurements of the temperature gradient inside them. By this way, the measurement errors on the temperature gradient, due to the thermal contact resistances between specimens and heating plates, can be eliminated. This procedure enables one to perform reliable guarded hot-plate measurements on materials having a thermal conductivity up to  $5 \text{ W}\cdot\text{m}^{-1}\cdot\text{K}^{-1}$ .

The aim of this work is to obtain a relative uncertainty on thermal-conductivity measurements better than 5 % in the considered temperature and thermal-conductivity ranges. This paper presents the main features of this new GHP apparatus and the first results of thermal-conductivity measurements performed at high temperature.

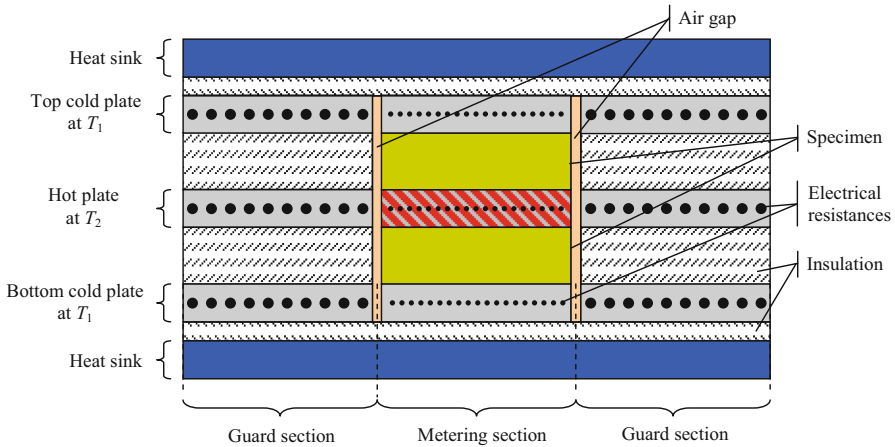


**Fig. 1** Cross-section view of LNE’s high-temperature guarded hot plate in a double-specimen configuration

## 2 Design of the Apparatus

### 2.1 Measurement Principle

The design of the setup is inspired from the classical guarded hot-plate configuration described in the EN 12667 and ISO 8302 standards, to ensure a steady, unidirectional, and uniform heat flow crossing the specimens. A temperature gradient is established through two specimens placed between two plates controlled at different temperatures (Fig. 1). In these conditions, the Fourier law can be applied giving the relationship

$$q = \frac{\varphi}{S} = \lambda \frac{\Delta T}{e}, \tag{1}$$

where  $\varphi$  is the electrical power supplied to the metering section (W),  $S$  is the area of the specimens ( $m^2$ ),  $\Delta T$  is the mean temperature drop across the specimens (K), and  $e$  is the mean thickness of the specimens (m).

The temperature drop  $\Delta T$  through the specimens is the temperature difference between their two surfaces:

$$\Delta T = T_2 - T_1, \tag{2}$$

where  $T_1$  is the average temperature of the cold surface (K) and  $T_2$  is the average temperature of the hot surface (K).

The mean temperature of the specimens  $T_m$  is defined as the mean value of  $T_1$  and  $T_2$ . The thermal conductivity is calculated using the relation

$$\lambda = \frac{\varphi}{S} \frac{e}{\Delta T}. \tag{3}$$

The basic concept and general features of the high-temperature apparatus are shown in Fig. 1.

## 2.2 Description of the Components

The different components of the GHP apparatus have been designed to perform thermal-conductivity measurements up to 800 °C. The main measurement difficulties at these temperature levels have been identified in the previous work [3,9].

- The mechanical and thermal properties of the heating plates are difficult to sustain at high temperatures, especially if the plates are submitted to several thermal cycles under air. The materials used to build the plates must have a high thermal conductivity and good resistance to oxidation. To get a good thermal uniformity and a good resistance to deflection under load, the thickness must be higher than for a room-temperature GHP, even if it leads to more parasitic heat fluxes around the metering section.
- The flatness of the plates has to be low enough in order to reduce effects of thermal contact resistances. Good flatness is difficult to maintain due to residual mechanical stresses introduced by machining. For that reason, the heating plates should undergo a specific procedure composed of a heat treatment after machining in order to release residual stresses, and a “soft” machining to obtain good flatness.
- The heating technologies are limited to the use of electrical resistance wires that are metal sheathed. But by this way, it is not possible to measure accurately the voltage of the “hot wires” at the entrance of the metering section. The voltage drop of the “cold wires” has to be estimated to get the effective voltage supplied to the metering section.
- High-temperature sensor technologies are less reliable and less accurate than at room temperature. In order to improve their resistance to oxidation, sensors are required to be metal sheathed and to have a bigger section. This can introduce further parasitic heat fluxes.

The main features of the new high-temperature GHP built by LNE are described hereafter.

### 2.2.1 Geometry and Size of Specimens

The use of circular specimens can be difficult for their preparation or machining. Even if a circular configuration can avoid some isothermal defaults existing in the corners of the metering section for a square geometry configuration [10], LNE chose the use of a square specimen configuration in order to ease the preparation of the specimens. It also enables one to answer manufacturer requests when it is not technologically possible to machine some kinds of materials in circular shapes.

The accurate configurations of guarded hot plates use a very wide metering section in order to have a high heat flux crossing the specimens compared to surrounding parasitic heat fluxes. In that case, large specimens (up to 1 m diameter) with parallel and very flat faces are required. It is usually difficult to prepare specimens attaining

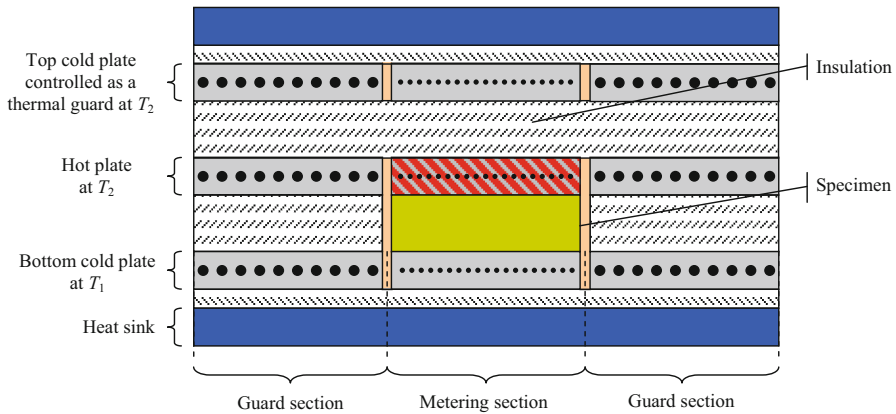


**Fig. 2** View of the GHP in a single-specimen configuration

these geometric specifications for materials used at high temperatures (rigid insulating materials, composites, ceramics, and polymers...). For that reason, the GHP apparatus presented here was designed to measure the thermal conductivity of one or two square specimens with rather a small size ( $100\text{ mm} \times 100\text{ mm}$ ) and a thickness varying from 10 mm to 80 mm.

The choice between a single or double-specimen configuration depends on their thermal conductivity. The lower the thermal conductivity of the specimens, the higher will be the accuracy using a double-specimen configuration instead of the single one. When the apparatus operates in the single-specimen configuration, the top specimen is replaced by an insulating material and the temperature of the top cold plate is controlled as a thermal guard (see Fig. 2). The single-specimen tested is usually placed at the bottom of the stack with the hot plate on its top face and the cold plate in contact with its bottom face. This procedure avoids convection effects by stratification of the air surrounding the specimen. In the case of insulating materials with soft surfaces such as fibrous materials that do not enable accurate square sampling (mineral wools or loose-fill materials...), the size of specimens is increased to  $320\text{ mm} \times 320\text{ mm}$ . They entirely cover the surface of the heating plates including the metering and the guard section. Measurements are then conducted in a double-specimen configuration in order to reduce parasitic heat fluxes of the top cold plate used as a thermal guard.

### 2.2.2 Design of the Heating Plates

The choice of the material constituting the three heating plates (one hot plate and two cold plates) is based on a compromise between the thermal conductivity, the resistance to oxidation, the ease of machining, and the geometrical stability after temperature cycling. These square heating plates ( $320\text{ mm} \times 320\text{ mm}$ ), shown in Fig. 3, are made of nickel 201 alloy (thermal conductivity:  $70\text{ W}\cdot\text{m}^{-1}\cdot\text{K}^{-1}$  to  $55\text{ W}\cdot\text{m}^{-1}\cdot\text{K}^{-1}$  from  $23\text{ }^\circ\text{C}$  to  $800\text{ }^\circ\text{C}$ ). The thickness, set to 32 mm, enables improvement of the mechanical

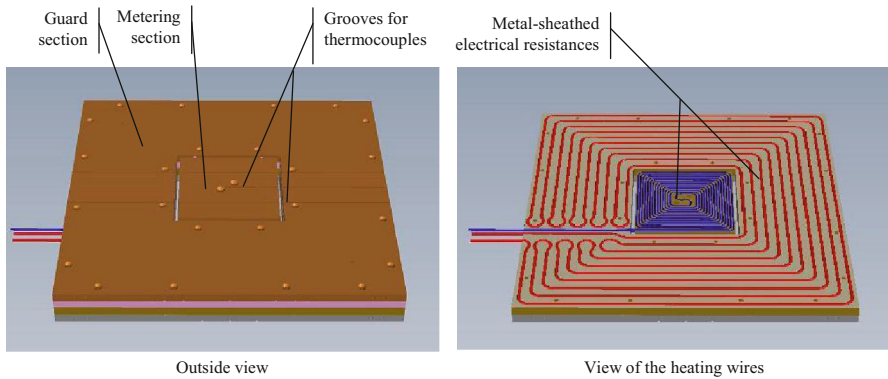


**Fig. 3** Scheme of the heating plate

resistance to deflection under load and to increase the thermal uniformity. The heating plates being very heavy (30 kg each), some counterweights enabling to set a pressure on the specimen surfaces from 0.5 kPa to 50 kPa, are used in order to avoid excessive compression of specimens.

The flatness of the plates was about 0.01 mm over the metering section at the end of the machining process in order to reduce thermal contact resistances between the specimens and the plates. The flatness defects create air gaps that introduce non-uniformity of the temperature at the faces of the specimens. These parasitic thermal resistances are implicitly included in the calculation of the thermal resistance of the specimen when temperatures used to determine the temperature drop are measured inside the heating plates. In order to limit the distortion of the plates due to mechanical stresses of the machining, the components constituting the heating plates have been heat-treated. The plates are electrically heated with metal-sheathed resistive wires embedded between two grooved nickel plates. The heating wires are regularly arranged to generate a uniform heat flux density through the specimen.

### 2.2.3 Guard Section

The purpose of the guard section is to ensure that the heat flux remains unidirectional in the metering section, simulating a semi-infinite wall behavior. The same temperature gradient is established in the insulating material surrounding the specimens and in the specimens, in order to ensure that all the powers supplied by the main heater unit go through the specimens. On the standardized large size guarded hot plates, the width of the guard rings is usually equal to half of the width of the metering section. At high temperature, the heat losses by the edges of the stack can be important, generating disturbances across the air gap and thus heat losses from the metering section. To minimize these edge effects, the guard rings of the LNE's apparatus are designed as wide as the metering section. So the heat losses through the air gap can be reduced, and the maximum acceptable thickness for the specimens can be increased.

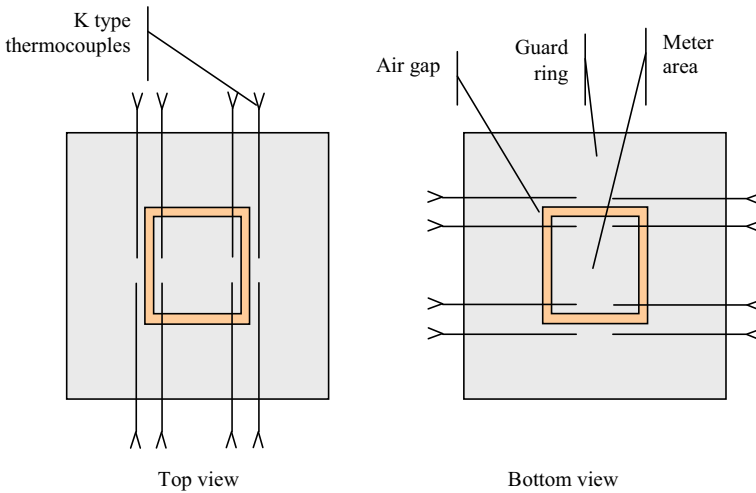


**Fig. 4** Schematic diagram of the thermopile arrangement in the heating plate

To achieve good control of the temperatures at the cold faces of the specimen and good thermal equilibrium around the specimens, the cold plates are also designed with independent metering and guard sections, as for the hot plate.

#### 2.2.4 Temperature Control

The metering sections are controlled with K-type metal-sheathed thermocouples connected to high-resolution (0.01 K) temperature controllers. The guard rings are temperature controlled to keep a zero temperature difference with the metering section. This difference of temperature is measured with a multi-junction differential thermopile across the air gap. It is constituted with sixteen K-type thermocouples located in the metering section mounted in a differential mode with eight other ones located in the guard section (see Fig. 4). This thermopile has a sensitivity of about  $320 \mu\text{V}\cdot\text{K}^{-1}$  that enables control of the balance of temperature with a resolution of about 0.01 K. The thermocouples of the thermopile are located around the edge of the metering section and on both faces of the plates in order to measure the mean temperature difference between the metering and guard sections. The external diameter of the thermocouples is 1.0 mm to minimize conduction heat fluxes across the gap.

#### 2.2.5 Air Gap

Measurements of the thermal conductivity using a GHP are usually performed with continuous specimens covering the whole plate (especially for low conductivity materials), including the metering and guard sections. LNE chose to operate with specimens having the same section as the metering unit, flatness defects being easier to control over the metering section only than over the whole plate. The air gap (4 mm wide) that surrounds the specimens aims to ensure their insulation against parasitic heat fluxes,

**Table 1** Relative weight of heat loss corrections due to the gap as a function of the thermal conductivity of specimens

Thermal conductivity ( $\text{W}\cdot\text{m}^{-1}\cdot\text{K}^{-1}$ )	Relative weight of the heat loss to the heat flow crossing the specimen (%)
0.107	1.95
0.291	0.73
0.380	0.53
0.556	0.38
1.190	0.20

especially for medium conductivity materials. It can be filled with an insulating and opaque loose-fill material in order to decrease the radiation heat transfer, which is the most important heat exchange mode across the air gap at high temperature. Nevertheless, residual heat transfers along the gap must be taken into account in the calculation of thermal conductivity. This correction can be important in the case of low conductivity materials, but becomes negligible for medium conductivity materials. Estimated values of the heat loss correction are presented in Table 1 as a function of the thermal conductivity measured.

### 2.2.6 Temperature Measurements

The temperature measurements of the faces of the specimens are performed with thin metal-sheathed K-type thermocouples (1.0 mm diameter). The average temperature of each specimen surface is measured using up to five sensors placed in grooves carved into the surfaces of the plates in contact with the specimens (see Fig. 3).

Despite the possible drift of their response when heated above 400 °C, K-type thermocouples have been selected due to their high sensitivity enabling good resolution for temperature drop measurements. The reliability of temperature measurements is insured by several sensors and by periodic calibrations. It would be possible to use small-diameter platinum resistance thermometers, but their operating temperature is generally limited to 400 °C.

The main drawback of the usual method, consisting of using temperatures measured in the plates to calculate the thermal conductivity, is the influence of the thermal contact resistances between the faces of the specimens and the plates. These parasitic thermal resistances are not negligible for materials with low thermal resistances. For such materials, it is preferable to measure directly the temperature gradient inside the specimens by introducing sensors in holes drilled at different known distances from their faces (see Fig. 5). It is possible with this new GHP to introduce twelve sensors in the specimens in order to measure the mean temperature gradient. The distance between the sensors must be known with an uncertainty better than 0.2 mm in order to reach the uncertainty expected for the thermal-conductivity measurements. This procedure enables simultaneous measurements of the thermal conductivity of the specimens and the temperature inside the heating plates, and thus to determine the thermal contact resistances between the heating plates and the specimens.



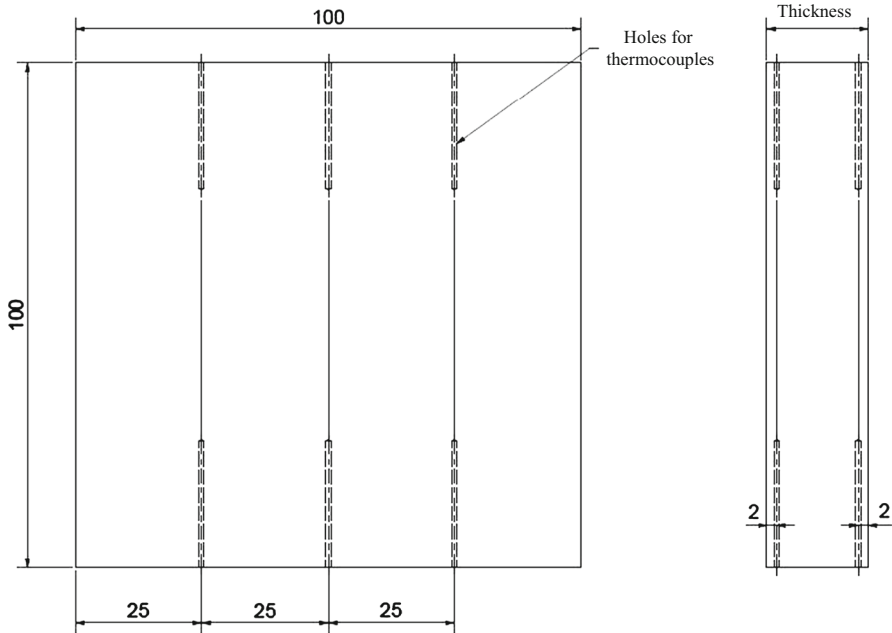


**Fig. 5** Drawing of the specimens machined in order to insert temperature sensors

### 3 Experimental Results

#### 3.1 Control of the Accuracy of the GHP Apparatus

The accuracy of the GHP apparatus is difficult to estimate at high temperatures by performing measurements with certified reference materials (CRMs) due to the lack of these materials [10, 11]. Only a few CRMs can be used for this study:

- Pyrex glass BCR039 [12]
- Resin-bonded glass fiber board IRMM440 [13].

Another way to control the accuracy of the GHP apparatus consists of using materials whose thermal conductivity has been measured with reference facilities based on absolute measurement methods. LNE developed some years ago complementary facilities for accurate measurements of the thermal conductivity using two different metrological approaches:

- GHP built according to ISO8302 and devoted to thermal-conductivity measurements of insulating materials from  $-20\text{ }^{\circ}\text{C}$  to  $80\text{ }^{\circ}\text{C}$  [14],
- Indirect method based on the assessment of thermal conductivity from the measurements of thermal diffusivity, specific heat, and density, for medium and high conductivity materials from  $23\text{ }^{\circ}\text{C}$  to  $1500\text{ }^{\circ}\text{C}$  [15].

These reference facilities were used in the first international interlaboratory comparisons on thermal-diffusivity and thermal-conductivity measurements organized by the

**Table 2** Reference values of “calibrated” or standard reference materials

Material	Calibration method	Thermal conductivity ( $\text{W}\cdot\text{m}^{-1}\cdot\text{K}^{-1}$ )	Temperature range ( $^{\circ}\text{C}$ )	Relative expanded uncertainty ( $k = 2$ )
Microporous insulating material	Room temperature GHP	0.028 to 0.030	23 to 60	2 %
Glass fiber board IRMM440	Certified reference material	0.0340	40	0.8 %
Composite with mineral charges	Indirect method	0.26	23	6 %
Composite with glass charges	Indirect method	0.44	23 to 75	7 %
Composite with carbon charges	Indirect method	0.76 to 0.79	23 to 75	7 %
Composite with borate charges	Indirect method	1.17	23	6 %
Pyrex glass BCR <sup>®</sup> – 039	Certified reference material	1.1 to 1.3	23 to 195	1.7 %
Granite	Indirect method	3.0	23	6 %
TA6V titanium alloy	Indirect method	6.9 to 15	23 to 600	4 %

Bureau International des Poids et Mesures (BIPM) [16, 17], and for the certification process of Pyroceram 9606 as BCR-724 reference material [18]. Several materials have been characterized using these techniques, and then used in the present work for the validation of the new high-temperature GHP apparatus by performing comparative measurements. Their thermal-conductivity and temperature ranges are presented in Table 2.

### 3.2 Measurements on Soft and Insulating Materials

The measurements were performed in a double-specimen configuration due to the very low conductivity of the tested materials. The size of the specimens was 320 mm  $\times$  320 mm, because it was not possible to shape correctly 100 mm  $\times$  100 mm specimens, which corresponds to the area involved in the thermal-conductivity calculation. In the case of 320 mm  $\times$  320 mm specimens, the effective area used to determine the thermal conductivity is the central area of the specimen, which is delimited by the center line of the gap of the hot plate. Measurements were carried out with a temperature drop of  $(15 \pm 5)$  K at 40  $^{\circ}\text{C}$  for the glass fiber board IRMM440, and at 23  $^{\circ}\text{C}$ , 35  $^{\circ}\text{C}$ , and 60  $^{\circ}\text{C}$  for a microporous insulating material (porous structure based on amorphous silica particles sized around 5 nm to 25 nm in diameter) with a density of 260  $\text{kg}\cdot\text{m}^{-3}$ . The relative deviations between the measured thermal conductivity and the reference values, shown in Table 3, are lower than 3.5 %. The test results obtained on the microporous insulating material show, however, that this relative deviation increases with temperature.

**Table 3** Thermal conductivity measured with the high-temperature GHP and relative deviations to reference values

Material	Thickness (mm)	Mean temperature (°C)	Thermal conductivity ( $\text{W}\cdot\text{m}^{-1}\cdot\text{K}^{-1}$ )	Relative deviation (%)
Microporous insulating material	22	23	0.0277	-2.7
		35	0.0283	-2.8
		60	0.0291	-3.3
Glass fiber board IRMM440	30	40	0.0348	2.4
Composite with mineral charges	20	23	0.252	-1.5
Composite with glass charges	10	23	0.413	-4.6
		75	0.427	-3.6
Composite with carbon charges	10	23	0.722	-4.7
		75	0.757	-4.5
Composite with borate charges	20	23	1.19	1.1
Pyrex glass BCR <sup>®</sup> – 039	19	23	1.14	-0.4
		50	1.18	0.5
		100	1.24	0.5
		150	1.29	0.5
		200	1.34	0.8
Granite	30	25	2.99	-2.2
TA6V titanium alloy	60	23	6.84	-1.4
		100	7.91	0.8
		200	9.30	4.3
		300	10.2	-0.1
		400	11.5	1.0
		500	12.9	3.7
		600	14.4	2.8

### 3.3 Measurements on Rigid and Medium Conductivity Materials

Measurements were performed in a single-specimen configuration on all rigid materials as shown in Table 2 having a thermal conductivity higher than  $0.2 \text{ W}\cdot\text{m}^{-1}\cdot\text{K}^{-1}$ . Specimens were machined according to the drawing shown in Fig. 5 and equipped with temperature sensors in order to avoid measurement errors due to thermal contact resistances. The temperature drops between specimen surfaces were set to  $(15 \pm 5) \text{ K}$  during the measurements.

The measurement results (given in Table 3) show relative deviations to the reference values less than 5 %, in accordance with the targeted uncertainty. Most of the relative deviations are less than 4 %, except for the thinnest specimens (10 mm thick) such as composites with glass charges or with carbon charges. This can be explained by the increase of the relative uncertainty on the distances between the sensors in the case of thin specimens. In addition, the uncertainty on the reference values of the thermal

**Table 4** Linearity assessment of the GHP

Temperature drop (K)	Thermal conductivity ( $\text{W}\cdot\text{m}^{-1}\cdot\text{K}^{-1}$ )	Relative deviation to “15 K temperature drop” (%)
10	0.0279	−1.12
15	0.0283	–
20	0.0282	−0.06
30	0.0280	−0.82

conductivity is higher for these composite materials because of their transparency to the laser used for the thermal-diffusivity measurements. However, it can be noticed in Table 3 that the relative deviation is lower than 1 % in the case of Pyrex Glass BCR039, for which reference values of the thermal conductivity are given with a very low uncertainty (see Table 2).

### 3.4 Linearity Assessment

The linearity of the GHP was evaluated using the microporous insulating material. This evaluation consists in verifying that the thermal resistance measured is independent of the temperature drop, for values ranging from 10 K to 30 K. The linearity assessment was performed by measuring the thermal conductivity at 35 °C for four temperature drops: (10, 15, 20, and 30) K. Measurement results are shown in Table 4, with a maximum relative deviation to “15 K temperature drop” equal to about 1 %.

### 3.5 Sources of Uncertainty

Several sources of uncertainties on thermal-conductivity measurements with high-temperature GHPs have been identified. Only the reproducibility of the apparatus and the most important uncertainty sources such as temperature and heat flux measurements are discussed in this paper.

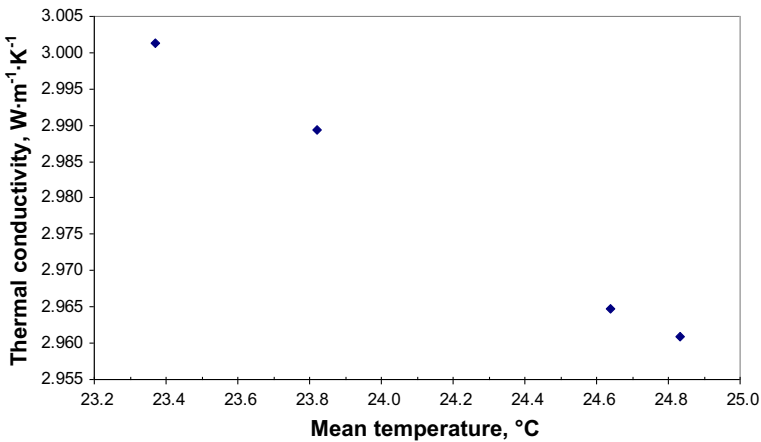
#### 3.5.1 Reproducibility of Measurements

The reproducibility of the new GHP of LNE was assessed by performing thermal-conductivity measurements on four granite specimens with very low geometry tolerances (parallelism and flatness, respectively, equal to  $\pm 0.02$  and  $\pm 0.01$ ). Measurements were carried out on different dates in a single-specimen configuration using the same measurement procedure (mean temperatures:  $(24 \pm 1)$  °C, mean temperature drop:  $(10 \pm 3)$  K, one specimen equipped with temperature sensors) and the same model of thermal-conductivity calculation.

The measurement results presented in Table 5 give a reproducibility better than 1 %. The mean test temperatures being not exactly the same for each specimen, the four thermal-conductivity values measured have been plotted as a function of temperature

**Table 5** Reproducibility control of the GHP

Specimen identification	Date of measurement	Mean temperature (°C)	Thermal conductivity ( $\text{W}\cdot\text{m}^{-1}\cdot\text{K}^{-1}$ )	Relative deviation to mean value (%)
Granite 1	05/2011	24.8	2.96	-0.61
Granite 2	11/2012	23.8	2.99	0.35
Granite 3	02/2013	23.4	3.00	0.75
Granite 4	11/2012	24.6	2.96	-0.48
Mean value	–	24.2	2.98	–

**Fig. 6** Thermal conductivity of the granite as a function of temperature

in Fig. 6. It shows that the reproducibility could be improved by taking into account the variation of the thermal conductivity of the granite with temperature.

### 3.5.2 Temperature Measurements

The uncertainty on the measurement of the specimen's mean temperature is not an important factor in the assessment of the overall uncertainty of the thermal-conductivity measurements because the thermal conductivity of the materials usually varies slowly with temperature. The accuracy of the temperature measurements is a more critical point for the temperature-drop measurement. For low temperature-drop values of about 10 K, the accuracy of the temperature measurement must be better than 0.5 K in order to achieve the uncertainty target of 5 % on the thermal-conductivity measurements.

In order to obtain this uncertainty level for temperature-drop measurements, it is necessary to carefully calibrate the temperature sensors.

- Sensors used for the temperature-drop measurement must be calibrated together in a block having a very uniform temperature, and

**Table 6** Sensitivity to the thermal equilibrium of the guard section

Temperature imbalance of the guard section (K)	Relative deviation to the heat flow measured for the 0 K temperature imbalance (%)	
	Insulating material <sup>a</sup>	Medium conductivity material <sup>b</sup>
−1	32.2	1.2
0	–	–
1	32.3	−1.1

<sup>a</sup> Microporous insulating material (13 mm thick, double-specimen configuration, mean temperature: 300 °C, thermal conductivity: 0.0338 W·m<sup>−1</sup>·K<sup>−1</sup>)

<sup>b</sup> Pyrex glass BCR039 (19 mm thick, double-specimen configuration, mean temperature: 100 °C, thermal conductivity: 1.24 W·m<sup>−1</sup>·K<sup>−1</sup>)

- Periodicity of the calibration must be adapted to the drift of the K-type thermocouples due to the heating at temperatures above 400 °C.

The non-uniformity of the temperature drop across the specimens during the thermal-conductivity measurements is also an uncertainty source. The flatness defects generate distortions of the temperature gradient due to the heterogeneous contact between the plates and the specimens. The uncertainty on the mean temperature drop, which is the main part of the uncertainty on thermal-conductivity measurements in the case of medium conductivity materials, is significantly reduced using several temperature sensors located inside the specimens (cf. Fig. 5).

### 3.5.3 Heat Flow Measurements

The uncertainty on the heat flow measurements is mainly due to

- Defects of thermal equilibrium of the guard rings: the guard rings ensure a zero temperature difference around the metering section in order to have a unidirectional heat flow through the specimens. Measurement results of the thermal conductivity are very sensitive to this thermal equilibrium. It depends on different parameters such as the air gap, the thickness of the specimens, its thermal conductivity, or the mean temperature. The sensitivity to the temperature difference between the metering and the guard section has been assessed by testing successively a very low and a medium conductivity material (microporous insulating material and Pyrex BCR039). The method applied to determine the sensitivity consists of setting the temperature difference between metering and guard sections at different values (such as −1 K, 0 K, and 1 K) and in measuring the heat flow supplied to the specimen. Obtained results presented in Table 6 show that the sensitivity of the low conductivity material to the thermal equilibrium of the guard section is thirty times higher than that of the medium conductivity material. In the case of a very low conductivity material, the temperature difference between the guard and metering sections must be lower than 0.15 K without considering the uncertainty on other measurement parameters, in order to be able to reach the expected uncertainty of 5 % on thermal-conductivity measurements.

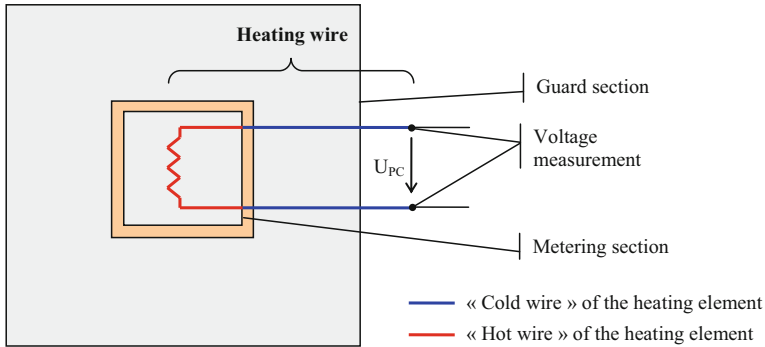


**Fig. 7** Measurement of the voltage drop across the heating wire

**Table 7** Uncertainty budget of the thermal-conductivity measurements for low thermally conductivity material (microporous insulating material:  $\lambda = 0.028 \text{ W}\cdot\text{m}^{-1}\cdot\text{K}^{-1}$  at 300 K)

Quantity $X_i$	Units	Estimate $x_i$	Relative variance $(u(x)/x)^2$	Relative weight (%)
Thickness ( $e$ )	m	22.00	$5.22 \times 10^{-5}$	3.7
Area ( $S$ )	$\text{m}^2$	0.022	$5.80 \times 10^{-6}$	0.4
Heat flow ( $\varphi$ )	W	0.790	$1.33 \times 10^{-3}$	93.6
Temperature difference ( $\Delta T$ )	K	29.80	$3.25 \times 10^{-5}$	2.3

- Correction of heat losses from the “cold wires”: For technological reasons, it is not possible (especially for the metal-sheathed heating elements) to measure directly the voltage drop across the “hot wire” of the heating element at the entrance of the metering section (see Fig. 7). The voltage measurement procedure introduces heat losses in the “cold wire” of the heating element that can be assessed from the knowledge of the electrical resistivity of the “hot” and the “cold” wires.

### 3.6 Assessment of Measurement Uncertainty

A first assessment of the measurement uncertainty has been performed at room temperature for two kinds of materials: an insulating material (microporous material) and a medium conductivity material (Pyrex BCR039). The uncertainty budget of the thermal-conductivity measurements is presented in Tables 7 and 8 for these two materials. For low conductivity materials, the most important uncertainty factor is the uncertainty on the heat flow measurement. It is due to the importance of the parasitic heat fluxes and heat losses compared to the level of the heat flow crossing the specimens. In the case of the medium conductivity material, the main source of uncertainty comes from the measurement of the temperature difference ( $\Delta T$ ), due to the uniformity defects generated by thermal contact resistances between the specimens and the plates.

The relative standard uncertainty ( $k = 1$ ) on the thermal conductivity  $\lambda$  is expressed by the quadratic sum of the relative measurement uncertainties of the electrical power

**Table 8** Uncertainty budget of thermal-conductivity measurements for medium thermally conductivity material (Pyrex BCR039:  $\lambda = 1.14 \text{ W}\cdot\text{m}^{-1}\cdot\text{K}^{-1}$  at 300 K)

Quantity $X_i$	Units	Estimate $x_i$	Relative variance $(u(x)/x)^2$	Relative weight (%)
Distance between sensors ( $e$ )	m	15.00	$1.59 \times 10^{-4}$	30.9
Area ( $S$ )	m <sup>2</sup>	0.010	$1.25 \times 10^{-5}$	2.4
Heat flow ( $\varphi$ )	W	19.48	$6.01 \times 10^{-5}$	11.7
Temperature difference ( $\Delta T$ )	K	10.50	$2.82 \times 10^{-4}$	55.0

$\varphi$ , the area of the specimens  $S$ , the temperature drop  $\Delta T$ , and the thickness of the specimens  $e$  (cf. Eq. 4), and these four uncertainty factors being considered to be independent.

$$\frac{u(\lambda)}{\lambda} = \sqrt{\frac{u^2(\varphi)}{\varphi^2} + \frac{u^2(e)}{e^2} + \frac{u^2(S)}{S^2} + \frac{u^2(\Delta T)}{\Delta T^2}}. \quad (4)$$

The relative expanded uncertainty ( $k = 2$ ) for the measurement of the thermal conductivity has been estimated to be 7.5 % for the low conductivity material (microporous insulating material) and 4.5 % for the medium conductivity material (Pyrex BCR039).

## 4 Conclusions

A new guarded hot-plate apparatus has been developed at LNE for thermal-conductivity measurements at high temperature. The metrological performances (reproducibility and linearity) of this facility have been evaluated, and its accuracy has been controlled by performing comparative measurements on “calibrated” and standard reference materials from 23 °C to 600 °C. The results obtained show relative deviations lower than the uncertainty target of 5 % for thermal-conductivity measurements over the whole thermal-conductivity and temperature ranges. An original procedure has been proposed for the measurement of the temperature drop across the specimen using several temperature sensors located inside the specimens. Errors due to thermal contact resistances between specimens and plates being avoided as a result of this procedure, it is possible to measure the thermal conductivity (up to  $15 \text{ W}\cdot\text{m}^{-1}\cdot\text{K}^{-1}$ ) of medium conductivity materials with this GHP.

## References

1. EN 12667, Thermal performance of building materials and products-determination of thermal resistance by means of guarded hot plate and heat flow meter methods-products of high and medium thermal resistance (2001)
2. ISO 8302:1991, Thermal insulation: determination of steady state thermal resistance and related properties: guarded hot plate apparatus (International Organization for Standardization, Geneva, Switzerland, 1991)



3. D.R. Flynn, R.R. Zarr, M.H. Hahn, W.M. Healy, ASTM Spec. Tech. Publ. 1426, 98 (ASTM, Conshohocken, PA, 2002), ISBN 0803128983
4. D.R. Salmon, R.P. Tye, A high temperature guarded hot plate intercomparison, in *Thermal Conductivity*, vol. 26 (DEStech Publications, Lancaster, PA, 2005), pp. 420–433, ISBN 1–932078-36-3
5. J.G. Hust, D.R. Smith, *Round-Robin Measurements of the Apparent Thermal Conductivity of Two Refractory Insulation Materials using High-Temperature Guarded-Hot-Plate Apparatus, NBSIR 88–3087* (National Bureau of Standards, Boulder, CO, 1988)
6. CEN/TS 15548–1, Thermal insulation products for building equipment and industrial installations: determination of thermal resistance by means of the guarded hot plate method. Part 1: Measurements at elevated temperatures from 100 °C to 850 °C (2011)
7. B. Hay, J. Hameury, N. Fleurence, P. Lacipière, M. Grelard, V. Scoarnec, G. Davée, *Int. J. Thermophys.* **35**, 1712 (2014). doi:[10.1007/s10765-013-1400-8](https://doi.org/10.1007/s10765-013-1400-8)
8. B. Hay, K. Anhalt, L. Chapman, K. Boboridis, J. Hameury, S. Krenek, L. Vlahovic, N. Fleurence, O. Beneš, *IEEE Trans. Nucl. Sci.* **61**, 2112 (2014)
9. D.R. Salmon, R.P. Tye, N. Lockmuller, *Meas. Sci. Technol.* **20**, 015101 (2009)
10. R.R. Zarr, Status of NIST thermal insulation reference materials, in *Thermal Conductivity*, vol. 29 (DEStech Publications, Lancaster, PA, 2008), pp. 120–128, ISBN 978-1-932078-72-5
11. R.R. Zarr, G.R. Dalton, S.M. Fioravante, Development of a NIST standard reference database for thermal conductivity of building materials, in *Thermal Conductivity*, vol. 25 (Technomic Publishing Company, Lancaster, PA, 1999), pp. 259–265, ISBN 1–56676-806-3
12. I. Williams, R.E. Shawyer, Certification report for a Pyrex glass reference material for thermal conductivity between –75 °C and 195 °C - CRM039, Report EUR 13358 (1991)
13. S. Quin, G. Venuti, F. de Ponte, A. Lamberty, Certification of a resin-bonded glass fibre board for thermal conductivity between –10 °C and +50 °C-IRMM-440, Report EUR 19572 EN (2000)
14. B. Hay, J. Hameury, J.-R. Filtz, F. Haloua, R. Morice, *High Temp.-High Press.* **39**, 181 (2010)
15. B. Hay, J.-R. Filtz, J. Hameury, L. Rongione, *Int. J. Thermophys.* **26**, 1883 (2005)
16. B. Hay, R. Zarr, C. Stacey, L. Lira-Cortes, U. Hammerschmidt, N. Sokolov, J. Zhang, J.-R. Filtz, N. Fleurence, *Int. J. Thermophys.* **34**, 737 (2013)
17. M. Akoshima, B. Hay, J. Zhang, L. Chapman, T. Baba, *Int. J. Thermophys.* **34**, 763 (2013)
18. B. Hay, L. Rongione, J.-R. Filtz, J. Hameury, *High Temp.-High Press.* **37**, 13 (2008)